

1
2
3
4
5
6
7
8
9
10
11
12
13
14
15
16
17
18
19
20
21
22
23
24
25
26
27

Decadal Variations of Intense Tropical Cyclones over the Western North Pacific during 1948-2010

Haikun Zhao, Liguang Wu and Ruifang Wang

Key Laboratory of Meteorological Disaster of Ministry of Education, China
Nanjing University of Information Science and Technology, Nanjing 210044, China

Corresponding author: Dr. Liguang Wu, liguang@nuist.edu.cn
Pacific Typhoon Research Center (PTRC)
Key Laboratory of Meteorological Disaster of Ministry of Education
Nanjing University of Information Science and Technology, Nanjing 210044

1. Introduction

The influence of global warming on tropical cyclone (TC) intensity has been extensively discussed over the past several decades (Emanuel 1987, 2005; Knutson et al. 1998, 2010; Knutson and Tuelya 2004; Bender et al. 2010). In the western North Pacific (WNP), studies suggested an increase in intense TCs (i.e. categories 4 and 5 in the Saffir-Simpson scale, hereafter Cat45) since the 1970s (Webster et al. 2005; Elsner et al. 2008), while longer TC records suggested that such an increasing trend in TC intensity is a part of interdecadal variations over the WNP basin (Chan 2006, 2008). Other studies indicated that the increasing Cat45 TCs since the 1970s was detected

28 only in the Joint Warning Typhoon Center (JTWC) best track dataset (Wu et al. 2006;
29 Kamahori et al. 2006; Song et al. 2010; Ren et al. 2011), suggesting substantial
30 uncertainty in historical TC intensity records. It is clear that understanding of possible
31 impacts of global warming on TC intensity is complicated by various natural
32 variations and uncertainty in historical TC data.

33 Some studies have been conducted on the decadal and interdecadal variations
34 in TC frequency and tracks over the WNP basin (Yumoto and Matsuura 2001;
35 Matsuura et al. 2003; Yumoto et al. 2003; Ho et al. 2004; Liu and Chan 2008; Kim et
36 al. 2010). Based on the Regional Specialized Meteorological Center of Tokyo (RSMC)
37 TC dataset since 1951, Yumoto and Matsuura (2001), Yumoto et al. (2003) and
38 Matsuura et al. (2003) found significant variations in TC frequency with a period of
39 about 20 years and suggested that the interdecadal variability was associated with
40 increased (decreased) sea surface temperature (SST) in the central and eastern
41 equatorial Pacific, which strengthens the tropical westerlies (easterlies), leads to the
42 eastward (westward) extension (retreat) of the monsoon trough and an anomalous
43 cyclonic (anticyclonic) circulation east of the Philippines and thus increasing
44 (decreasing) annual TC frequency. Ho et al. (2004) contrasted the track change
45 between the two periods of 1951-1979 and 1980-2001 with the JTWC best track data
46 and linked the interdecadal change to the westward expansion of the North Pacific
47 subtropical high. Liu and Chan (2008) also suggested a significant interdecadal
48 variability of the TC tracks in the WNP basin during the period 1960-2005. Based on
49 a TC trajectory model, Wu et al. (2005) showed that two prevailing TC tracks in the

50 WNP basin have shifted westward significantly over the past four decades due mainly
51 to changes in large-scale steering flows while TC activity in the South China Sea
52 decreased.

53 However, relatively few studies have examined TC intensity changes in the
54 WNP basin on the decadal and interdecadal time scales. Using the JTWC best track
55 data during the period of 1960-2005, Chan (2006, 2008) showed prominent
56 interdecadal variations in the frequency of Cat45 TCs with a period of about 18-32
57 years and argued that the variability was due to changes in the thermodynamcial and
58 dynamical factors (e.g., SST, low-level vorticity, moist static energy and vertical wind
59 shear), while Wu and Wang (2008) argued that changes in the proportion of the Cat45
60 TCs over the past three decades were associated with changes in TC formation
61 locations and prevailing tracks. Furthermore, some studies suggested that TC
62 maximum wind speeds in the JTWC dataset before 1973 were overestimated
63 (Emanuel 2005, 2007). Currently, the uncertainty involved in these datasets has
64 become an important issue in understanding of the possible influence of global
65 climate change on TC activity in the WNP basin. Given considerable uncertainty in
66 historical TC records, one question arises as to whether there are significant decadal
67 and interdecadal variations of Cat45 TCs in the WNP basin, which is the main
68 objective of this study. The knowledge gained from such an analysis may help to
69 improve our understanding of the decadal variation of Cat45 TC frequency and
70 provide important background and useful predictors for improving its potential of
71 decadal prediction.

72 The rest of the paper is organized as follows. The datasets and processing used
73 in this study are described in Section 2. The methodology and dynamically-derived
74 climate changes in the basin-wide Cat45 TC frequency are presented in Section 3. The
75 controlling factors for decadal variability of Cat45 TC frequency are identified in
76 Section 4 and the associated large-scale pattern is investigated in Section 5. A brief
77 summary is given in Section 6.

78 **2. Datasets and Processing**

79 The monthly SST is from the National Oceanic and Atmosphere Administration
80 (NOAA) reconstructed SST (version 3) with horizontal resolution of $2^{\circ} \times 2^{\circ}$ (Smith
81 and Reynolds 2004). The wind data is obtained from the National Centers for
82 Environmental Prediction-National Center for Atmospheric Research (NCEP-NCAR)
83 reanalysis dataset with horizontal resolution of $2.5^{\circ} \times 2.5^{\circ}$ (Kalnay et al. 1996). The
84 TC information from the JTWC best track dataset includes TC center positions and
85 intensity at six-hour intervals in the WNP basin. Wu and Zhao (2011) indicated that
86 JTWC dataset is more reliable compared to other TC best track datasets available in
87 the basin. Chan (2008) also argued that the intensity records from the JTWC dataset
88 are relative reliable. For this reason, we use the JTWC dataset as the observation in
89 this study. In the JTWC best track dataset, TC intensity was mainly estimated from
90 aircraft reconnaissance in the pre-satellite era, which started around 1945, but was
91 discontinued in 1987 (Landsea et al. 2006). Since then, the Dvorak technique that was
92 developed during the 1970s has been used to estimate TC intensity from satellite
93 imagery and other satellite-based measurements (Dvorak 1975; Landsea 2007). The

94 evolution of the technique of TC intensity estimating can lead to inhomogeneity in the
95 TC intensity records and thus caution should be taken to address long-term variations
96 in TC intensity.

97 Emanuel (2005) extensively discussed that the evolution in measurement and
98 estimation techniques introduces in historical records of TC wind speeds.
99 Subsequently, Emanuel (2007) provided additional evidence supporting the need for a
100 downward adjustment of intensities in the early part of record using the refined
101 combined wind-pressure relationship in Emanuel (2005), and in agreement with
102 Landsea's (1993) earlier analysis. In the present study, following Emanuel (2005,
103 online supplement), we first adjust the maximum wind speeds in the JTWC dataset
104 prior to 1973. As shown in Fig.1, the annual TC number is reduced prior to the 1970s
105 after the adjustment. The annual Cat45 TC frequency is also substantially reduced
106 prior to the 1970s (Fig.2a). As a result, the heightened Cat45 TC activity around 1960
107 in the historical (hereafter unadjusted) TC intensity records, which was argued as a
108 peak of the interdecadal variations (Chan 2006, 2008), vanishes in the adjusted TC
109 intensity time series. Instead pronounced decadal variations of the annual Cat45 TC
110 frequency can be found, with most prominent peaks occurring around 1969, 1991 and
111 2004 (Fig. 2a).

112 Variations in the adjusted and unadjusted Cat45 TC frequencies during the
113 period 1948-2010 are examined with a spectral analysis. As shown in Figs. 3a and 3b,
114 all the unadjusted, adjusted and simulated Cat45 TC frequencies show interannual
115 cycles although their significant spectral peaks are not exactly the same. On the

116 decadal scale, a significant spectral peak is about 25 years in the unadjusted Cat45 TC
117 frequency, while 12-18 years cycle can be found in the adjusted and simulated Cat45
118 TC frequency. Although the edge effects in spectral analysis, it is found that the
119 results are robust because the significant periods are essentially the same when we use
120 the wavelet analysis (Figures not shown). Zhao et al. (2011) suggested that
121 interannual variations in TC intensity are dominated by the interannual variability of
122 the monsoon trough associated with SST changes, but the associated physical
123 mechanisms of the decadal variations of Cat45 TC frequency are not well understood
124 in the literature, due mainly to short TC records and uncertainty in historical intensity
125 records.

126 **3. Methodology and Numerical simulations**

127 Recently, an approach was used to assess historical TC intensity records (Wu
128 and Zhao 2012). In the approach, the intensity of each storm is numerically simulated
129 with a TC intensity model (Emanuel et al. 2006; Emanuel et al. 2008). Using this
130 approach, Wu and Zhao (2012) found that the evolution of the basin-wide TC
131 intensity in the JTWC best track dataset can be reasonably well simulated over the
132 period of 1975-2007. In addition, they suggested that the Cat45 TC frequency is
133 sensitive to changes in the vertical wind shear (VWS) and SST. For this reason, here
134 we focus on the annual Cat45 TC frequency and conduct numerical simulations
135 similar to those in Wu and Zhao (2012) by extending the study period back to 1948.

136 The TC intensity model is an axisymmetric numerical atmospheric model,
137 coupled with a simple one dimensional ocean model (Emanuel 2006; Emanuel et al.

138 2008). Using the intensity model, Emanuel et al. (2008) explored the influence of
139 various environmental factors on TC intensity. In this study, the observed TC tracks
140 during the period of 1948-2010, and the corresponding VWS and SST along the TC
141 tracks are supplied. The VWS is calculated as the magnitude of the monthly vector
142 difference between 850 hPa and 200 hPa. and its effect is parameterized in the TC
143 intensity model. Note that the influence of SST changes associated with TC-ocean
144 interaction is not included in this study. All of the observed TCs in the JTWC dataset
145 are allowed to move along the observed TC tracks and their intensity evolution is
146 simulated in the intensity model. The intensity model is initialized with a warm-core
147 cyclonic vortex. The maximum wind speed of the initial vortex is set to be 21 m s^{-1}
148 after a series of numerical experiments because the model vortex weakens at the
149 beginning of the simulation, which was also adopted in Wu and Zhao (2012) and Zhao
150 et al. (2011). Note that the intensity of the initial vortex has a little influence on our
151 simulations, very similar patterns and temporal variations except for the magnitude of
152 TC intensity when we conducted a few sensitivity experiments. The other parameters
153 of the initial vortex are the same as those in Emanuel et al. (2008). The same model
154 setup is used for all the simulation in this study and the Student's t-test method is used
155 to test the statistical significance at the 95% confidence level (Wilks 1995).

156 In the control experiment (CTRL) (Table 1), all of the TCs move with their
157 observed tracks, experiencing the corresponding observed monthly VWS and SST
158 along the TC tracks during the period 1948-2010. As shown in Fig.2a, the simulated
159 Cat45 TC frequency is in good agreement with the adjusted Cat45 frequency. The

160 correlation coefficient is 0.86 during the period 1948-2010, statistically significant
161 with an effective sample size of 51, which is referred to Dawdy and Matalas (1964).
162 As shown in Fig.3c, the significant spectral peaks in the simulated Cat45 TC
163 frequency are about 2.5, 4, 5, 9 and 15 years. In agreement with the adjusted Cat45
164 frequency, the 18-32 year variability is not statistically significant in the simulated
165 Cat45 TC frequency, suggesting that the 18-32 year variability is due mainly to the
166 different wind-pressure relationships used in the JTWC records during the period
167 1948-2010.

168 Given the observed TC tracks used in the simulation, uncertainty in the
169 simulation may result from missed or incomplete TC track records in the JTWC
170 dataset, especially during the pre-satellite era (Landsea 2007). To demonstrate it, the
171 JTWC best track data are divided into three periods: 1948-1964, 1965-1972 and 1973
172 -2010, which are based primarily on the development in the observational techniques.
173 In 1965 satellite data started to be used to monitor TCs (Landsea 2007; Emanuel 2008)
174 and a new wind-pressure relationship was used for estimating TC intensity since 1973
175 (Emanuel 2005). Here the average TC lifetime and the average time for a TC to
176 achieve Cat45 intensity are examined. For the three periods, the average lifetime of
177 the Cat45 TCs is 6.68, 8.25 and 8.84 days while the mean time to taking to achieve
178 Cat45 intensity is 2.61, 3.13, 3.30 days, respectively. Further calculations suggested
179 that the mean lifetime during the pre-satellite period is indeed significantly shorter
180 than the two post-satellite periods, indicating incomplete track records in the JTWC
181 dataset during the pre-satellite period. Moreover, the Cat45 TCs had relatively short

182 lifetime in the pre-satellite era.

183 However, the adjusted Cat45 TC frequency prior to the satellite era may be
184 reasonable. First, in the presence of aircraft reconnaissance during 1948-1972 and
185 relatively long duration, Cat45 TCs should have less chance to be missed in the JTWC
186 dataset than weak TCs. Second, the locations of reaching Cat45 intensity occurred
187 mostly in the western part of the WNP basin, and could be covered by the aircraft
188 reconnaissance stationed in Guam (Fig. 4).

189 In addition, the simulated Cat45 TC frequency is well consistent with the one in
190 the adjusted dataset. Despite the relatively short duration in the pre-satellite era, both
191 of the simulated and adjusted Cat45 TCs show a similar rapid intensification process.
192 It is note that the simulated TC intensification is smaller than the observation (Wang
193 and Zhou 2008). On average, the observed (simulated) Cat45 TCs take 48 hours to
194 increase about 32 m s^{-1} (23 m s^{-1}) in the maximum wind before reaching Cat45
195 intensity during the period 1973-2010. The average time for a TC to achieve Cat45
196 intensity in the model is about 3.3 days, which also compares well with the
197 observation. Associated with the lifetime of 6.68 days in the pre-satellite, it has
198 enough time to allow TCs to reach the Cat45 intensity in the model.

199 **4. Identification of the controlling factors for decadal variability**

200 As shown in Fig. 2a, the adjusted records and simulation clearly show that the
201 frequency of Cat45 TCs persistently increased with a nearly linear trend over the past
202 60 years although the simulated trend is smaller than the adjusted. While further study
203 is needed to verify the increasing trend, here we focus on the decadal variability of the

204 Cat45 TC frequency. For this purpose, all variables in the following discussion have
205 been detrended to reduce the influence of the long-term trend and a 5-year running
206 average is also used to reduce the interannual influences. The influences of SST and
207 VWS on the climate change of TC intensity were extensively discussed in previous
208 studies (Goldenberg et al. 2001; Emanuel 2005, 2008; Webster et al. 2005; Wu et al.
209 2008; Zhao et al. 2011; Wu and Zhao 2012). Wu and Wang (2008) suggested that
210 changes in the basin-wide TC intensity can be associated with shifts of the prevailing
211 TC tracks. Here we examine the individual contributions of changes in TC tracks,
212 SST and VWS to the decadal variability of Cat45 TC frequency by conducting three
213 sensitivity experiments.

214 As shown in Table 1, Experiment T-Clim (V-Clim) is the same as the CTRL,
215 but with the SST (VWS) along the TC tracks using the climatological mean during the
216 period of 1948-2010, while experiment VT-Clim is run with both of the SST and
217 VWS that are fixed in the climatological mean environment. Examination indicates
218 that the simulated annual Cat45 TC frequency in the three sensitivity experiments are
219 well correlated with that in the CTRL experiment (correlation coefficients all exceed
220 0.8) (Fig.5a), suggesting that neither SST nor VWS is the primary controlling factor
221 for the decadal variations (Fig.5a). The influence of SST (VWS) changes on the
222 decadal variability of the basin-wide Cat45 TC frequency can be obtained by
223 contrasting V-Clim (T-Clim) and VT-Clim, respectively. As shown in Fig.5b, it is
224 found that the simulated difference of Cat45 TC frequency between them is weakly
225 correlated with the CTRL (both the correlation coefficients are about 0.09), also

226 suggesting that SST (VWS) change has little direct influence on the decadal
227 variability of Cat45 TC frequency. However, the combined effect of SST and VWS
228 changes, which is examined by contrasting CNTL and the difference between CNTL
229 and VT-Clim, is much larger than the sum of their individual contributions (Fig.6a).
230 Its correlation with the simulated Cat45 frequency is 0.35, significant at a 95%
231 confidence level. This indicates that the combination of SST and VWS changes
232 contributes to the decadal variability in the basin-wide Cat45 TC frequency.

233 Wu and Wang (2008) suggested that the shifts in the TC prevailing tracks may
234 have allowed more TCs to follow a longer journey that favors the development of
235 intense TCs. In this study, the effect of the TC track change can be derived by
236 contrasting the Cat45 TC frequencies between CTRL and VT-Clim. As shown in
237 Fig.6b, both of them are well correlated with a correlation coefficient of 0.82,
238 suggesting that the track change can nearly account for the decadal evolution of the
239 basin-wide Cat45 TC frequency, in part because of the combined effect of SST and
240 VWS change.

241 **5. The associated large-scale pattern**

242 As indicated above, numerical results suggest the change in TC tracks exhibit
243 the dominant influence on the decadal variability of Cat45 TC frequency over the
244 WNP basin. In order to understand how track changes can affect the decadal
245 variations of Cat45 TC frequency, as shown Fig. 2b, we contrast the large-scale
246 patterns between positive phases (1952-1957,1965-1973,1988-1996 and 2001-2006)
247 and negative phases (1950-1951,1958-1964,1974-1987, 1997-2000 and 2007-2008).

248 In this section, we mainly focus on the associated large-scale patterns between
249 positive and negative phases since 1965. It is mainly because satellite data started to
250 be used in locating TC centers in 1965 so that TC track information in the best track
251 data during the period is relatively reliable.

252 Figure 7 shows the differences in the TC formation frequency between the
253 positive and negative phases. Compared to the negative phases, the TC formation is
254 enhanced in the southeast part of the WNP basin (10° - 20° N, 135° - 170° E) in a positive
255 phase with a moderate decrease over the northwest part (10° - 25° N, 120° - 135° E). Note
256 that although some TCs over the WNP basin might be missed in the JTWC best track
257 data before the satellite era, we find that the composite difference of TC genesis
258 frequency between the positive and negative phases is similar when we use the data
259 since 1948. This suggests that TC formation locations shift eastward during the
260 positive phases, which is also indicated in the mean TC duration. For each individual
261 year, the mean duration is defined by the averaged duration of all TCs that occurred in
262 the peak TC season (July-September). The mean duration is 5.9 days for the positive
263 phases, which is significantly longer than 4.5 days for the negative phases.

264 We further calculate the correlations between SST and the adjusted Cat45 TC
265 frequency. A similar correlation pattern over the tropical central and eastern Pacific
266 can be found for the periods 1965-2010 and 1948-2010, respectively (Fig. 8). It is
267 clearly suggested that the increased Cat45 TC activity in the positive phases is closely
268 associated with SST changes over the tropical central and eastern Pacific. Figure 9
269 shows the differences of the 850 hPa winds and SST between the positive and

270 negative phases during the peak TC activity season since 1965. Similarly, we also
271 found similar large-scale pattern between the positive and negative phases when we
272 use the data from 1948 to 2010 (Figure not shown). To the west of the positive SST
273 differences, westerly wind differences extend from the Philippines Sea to 170°E.
274 Yumoto and Matsuura (2001), Yumoto et al. (2003) and Matsuura et al. (2003)
275 suggested that increased (decreased) SST in the central and eastern equatorial Pacific
276 strengthens the tropical westerlies (easterlies), leads to the eastward (westward)
277 extension (retreat) of the monsoon trough. The eastward extension of the monsoon
278 trough can be considered the response to the heating associated with the warming SST
279 anomalies (Gill 1980; Holland 1995).

280 Ritchie and Holland (1999) found that more than 75% of TCs in the WNP basin
281 are associated with the monsoon trough. Previous studies have found that TCs tend to
282 form near the eastern end of the monsoon trough (Holland 1995; Briegel and Frank
283 1997; Ritchie and Holland 1999). Therefore we can conclude that the atmospheric
284 response to the warming SST over the tropical central and eastern Pacific leads to the
285 eastward extension of the monsoon trough, providing a favorable large-scale
286 environment for TC formation and resulting in the eastward shift in TC formation
287 locations. As suggested by Wu and Wang (2008), the eastward shift in the TC
288 formation locations allows more TCs to follow a longer journey that favors the
289 development of Cat45 TCs, compared to the negative phases.

290 **6. Summary**

291 Using the JTWC best track data during the period 1948-2010, this study

292 examines the decadal and interdecadal variations of Cat45 TCs in the WNP basin and
293 the associated mechanisms. The basin-wide annual Cat45 TC frequency is
294 numerically simulated in a TC intensity model by allowing all of the observed TCs to
295 move along the observed TC tracks. The simulated annual Cat45 TC frequency is in
296 good agreement with the observation when the TC intensity prior to 1973 is adjusted
297 with the combined wind-pressure relationship as in Emanuel (2005). The simulated
298 and adjusted time series show decadal variations with three peaks around 1969, 1991
299 and 2004. Although the interdecadal variability with an 18-32 year period is found in
300 the unadjusted Cat45 TC frequency during the period 1948-2010, it is insignificant in
301 the simulated and adjusted Cat45 TC frequency. We argue that that the interdecadal
302 variability in Chan (2006, 2008) is due mainly to the different wind-pressure
303 relationships used in the JTWC records prior to 1973.

304 Numerical results show that changes in TC tracks is the most important factor
305 for the decadal variations in the Cat45 TC frequency although the combined effect of
306 changes in SST and VWS also contributes to the decadal variability. Further analysis
307 suggests that the decadal fluctuations in TC tracks are closely associated with
308 eastward shift in the TC formation locations. The warming SST over the tropical
309 central and eastern Pacific leads to the eastward extension of the monsoon trough and
310 then the eastward shift in TC formation locations. As suggested by Wu and Wang
311 (2008), the eastward shift in the TC formation locations favors more TCs having a
312 longer journey and having more chance for the development of Cat45 TCs.

313 It should be noted that the adjusted records and simulation clearly show that the

314 frequency of Cat45 TCs persistently increased with a nearly linear trend over the past
315 63 years although the simulated trend is smaller than the adjusted. As suggested in Wu
316 and Wang (2004) and Wu et al. (2005), long-term changes in prevailing TC tracks in
317 the WNP basin have been identified, which may have contributed to the increase of
318 the Cat45 TC frequency. Previous studies also argued that local SST change had
319 contributed to the increasing trend of TC intensity in WNP (Emanuel 1987; Knutson
320 et al. 1998; Knutson and Tuleya 2004; Bender et al. 2010). Furthermore, a recent
321 statistical analysis indicates that the observed TC track changes in WNP are linked to
322 global SST warming (Wang et al. 2011). However, the long-term increasing trend may
323 subject to uncertainty in TC historical data and further study is needed.

324 **Acknowledgments.** This research was jointly supported by the Natural Science
325 Foundation of the Jiangsu Higher Education Institutions (11KJB170009), the typhoon
326 research project (2009CB421503), the social commonweal research program of the
327 Ministry of Science and Technology of the People's Republic of China
328 (GYHY200806009), the Key Laboratory of Meteorological Disaster of Ministry of
329 Education Program(KLME1204) and the Priority Academic Program Development of
330 Jiangsu Higher Education Institutions(PAPD).

331 **References**

332 Bender, M. A., Knutson, T. R., Tuleya, R. E., Sirutis , J. J., Vecchi , G. A., Garner, S.
333 T., and Held, I. M, 2010:.. Modeled impact of anthropogenic warming on the
334 frequency of intense Atlantic hurricanes. *Science*, **327**, 454-458.

335 Briegel, L. M., and W. M. Frank, 1997: Large-scale influences on tropical

336 cyclogenesis in the western North Pacific. *Mon. Wea. Rev.*, **125**,1397-1413.

337 Chan, J. C. L., 2006: Comments on “Changes in tropical cyclone number, duration,
338 and intensity in a warming environment”. *Science*, **311**, 1713.

339 Chan, J. C. L., 2008: Decadal variations of intense typhoon occurrence in the western
340 North Pacific. *Proc. R. Soc. A.*, **464**, 249-272, doi:10.1098/rspa.2007.0183.

341 Dawdy, D. R., and N.C. Matalas, 1964: Statistical and probability analysis of
342 hydrologic data, Part III: Analysis of variance, covariance and time series, in
343 *Handbook of Applied Hydrology: A Compendium of Water Resources*
344 *Technology*, edited by V. T. Chow, pp, 868-890, McGraw Hill, New York.

345 Dvorak, V. F., 1975: Tropical cyclone intensity analysis and forecasting from satellite
346 imagery. *Mon. Wea. Rev.*, **103**, 420-430.

347 Emanuel, K. A., S. Ravela, E. Vivant and C. Risi., 2006: A Statistical-Deterministic
348 Approach to Hurricane Risk Assessment. *Bull. Amer. Meteor. Soc.*, **87**,
349 299–314.

350 Emanuel, K. A., 1987: The dependence of hurricane intensity on climate. *Nature*, **326**,
351 483–485.

352 Emanuel, K. A., 2005: Increasing destructiveness of tropical cyclones over the past 30
353 years. *Nature*, **436**, 686-688.

354 Emanuel, K. A., 2006: Climate and tropical cyclone activity: A new model
355 downscaling approach. *J. Climate*, **19**, 4797-4802.

356 Emanuel, K. A., 2008: The hurricane-climate connection. *Bull. Amer. Meteor. Soc.*, **89**,
357 ES10-ES20.

358 Emanuel, K. A., R. Sundararajan, and J. Williams, 2008: Hurricanes and global
359 warming: Results from downscaling IPCC AR4 simulations. *Bull. Amer.*
360 *Meteor. Soc.*, **89**, 347-367.

361 Elsner, J. B., J. P. Kossin, and T. H. Jagger, 2008: The increasing intensity of the
362 strongest tropical cyclones. *Nature*, **455**, 92-95.

363 Gill, A. E., 1980: Some simple solutions for heat-induced tropical circulation. *Quart.*
364 *J. Roy. Meteor. Soc.*, **106**, 447-462.

365 Goldenberg S. B., Landsea C. W., Mestas-Nunez, A. M., and Gray W. M., 2001: The
366 recent increase in Atlantic hurricane activity: causes and implications. *Science*,
367 **293**, 474–478.

368 Ho, C. H., J. J. Baik, J. H. Kim, D.Y. Gong, and C. H. Sui, 2004: Interdecadal changes
369 in summertime typhoon tracks. *J. Climate*, **17**, 1767-1776.

370 Holland, G. J., 1995: Scale Interaction in the Western Pacific Monsoon. *Meteorol.*
371 *Atmos. Phys.*, **56**, 57-79.

372 Kamahori, H. N., N. Yamazaki, N. Mannoji, and K. Takahashi, 2006: Variability in
373 intense cyclone days in the western North Pacific. *SOLA*, **2**, 104–107,
374 doi:10.2151/sola.2006-0271.

375 Kalnay, E., and Coauthors, 1996: The NCEP/NCAR 40-Year Reanalysis Project. *Bull.*
376 *Amer. Meteor. Soc.*, **77**, 437-471.

377 Kim, J. H., C. H. Ho, and P. S., Chu, 2010: Dipolar redistribution of summertime
378 tropical cyclone genesis between the Philippine Sea and the northern South
379 China Sea and its possible mechanisms. *J. Geophys. Res.*, 115, D06104,
380 doi:10.1029/2009JD012196..

381 Knutson, T. R., Tuleya, R. E. and Kurihara, Y, 1998: Simulated increase of hurricane
382 intensities in a CO₂-warmed climate. *Science*, **279**, 1018-1020.

383 Knutson, T. R., and Tuleya, R. E, 2004: Impact of CO₂-induced warming on
384 simulated hurricane intensity and precipitation: Sensitivity to the choice of
385 climate model and convective parameterization. *J. Climate* **17**, 3477-3495.

386 Knutson, T. R., J. L. McBride, J. Chan, K. Emanuel, G. Holland, C. Landsea, I. Held,
387 J. P. Kossin, A. K. Srivastava, and M. Sugi, 2010: Tropical cyclones and
388 climate change. *Nature Geoscience*, **3**, 157-163.

389 Landsea, C. W., 1993: A climatology of intense (or major) Atlantic hurricanes. *Mon.*
390 *Wea. Rev.*, **121**, 1703-1713.

391 Landsea, C. W., B. A. Harper, K. Hoarau, and J. A. Knaff, 2006: Can we detect trends
392 in extreme tropical cyclones? *Science*, **313**, 452-454.

393 Landsea, C. W., 2007: Counting Atlantic Tropical Cyclones back to 1900. *Eos Trans.*
394 *AGU*, **88**, 197-202.

395 Liu, K. S., and J.C.L.Chan, 2008: Interdecadal variability of western North Pacific
396 tropical cyclone tracks. *J. Climate*, **21**, 4464-4476.

397 Matsuura T, Yumoto M, S. Iizuka, 2003: A mechanism of interdecadal variability of
398 tropical cyclone activity over the western North Pacific. *Clim.Dyn.*,
399 **21**,105-117.

400 Ren, F., J. Liang, G. Wu, W. Dong, X. Yang, 2011: Reliability Analysis of Climate
401 Change of Tropical Cyclone Activity over the Western North Pacific. *J.*
402 *Climate*, **24**, 5887–5898.

403 Ritchie, E. A. and G. J. Holland, 1999: Large-Scale Patterns Associated with Tropical
404 Cyclogenesis in the Western Pacific. *Mon. Wea. Rev.*, **127**, 2027-2043.

405 Song, J.-J., Y. Wang, and L. Wu, 2010: Trend discrepancies among three best track
406 data sets of western North Pacific tropical cyclones, *J. Geophys. Res.*, **115**,
407 D12128, doi: 10.1029/2009JD013058.

408 Smith, T. M., and R. W. Reynolds, 2004: Improved extended reconstruction of SST
409 (1854-1997). *J. Climate*, **16**, 149-1510.

410 Webster, P. J., G. J. Holland, J. A. Curry, and H. R. Chang, 2005: Changes in tropical

411 cyclone number, duration, and intensity in a warming environment. *Science*,
412 **309**, 1844–1846.

413 Wang, B., and X. Zhou, 2008: Climate variability and predictability of rapid
414 intensification in tropical cyclones in the western North Pacific. *Meteor. Atmos.*
415 *Phys.*, **99**, 1-16.

416 Wang, R., L. Wu, and C. Wang, 2011: Typhoon track changes associated with global
417 warming. *J Climate*, **24**, 3748-3752.

418 Wilks, D. S., 1995: Statistical Methods in the Atmospheric Sciences. Academic Press,
419 467pp.

420 Wu, L. and B. Wang, 2004: Assessing impacts of global warming on tropical cyclone
421 tracks. *J. Climate*, **17**, 1686-1698.

422 Wu, L., B. Wang, and S. Geng, 2005: Growing influence of Typhoon on East Asia.
423 *Geophys. Res. Lett.*, **32**, L18703, doi: 10.1029/2005GL022937.

424 Wu, L. and B. Wang, 2008: What has changed the proposition of intense hurricanes in
425 the last 30 years? *J. Climate*, **21**, 1432-1439.

426 Wu, L., B. Wang, and S. A. Braun, 2008: Implications of tropical cyclone power
427 dissipation index. *Int. J. Climatol.*, **28**, 727-731.

428 Wu, L. and H. Zhao, 2012: Dynamically-Derived Tropical Cyclone Intensity Changes
429 over the Western North Pacific, *J. Climate*, **25**, 89-98.

430 Wu, M.-C., K.-H. Yeung, and W. L. Chang, 2006: Trends in western North Pacific
431 tropical cyclone intensity, *Eos Trans. AGU*, **87**, 537-538.

432 Yumoto, M., T., Matsuura, 2001: Interdecadal variability of tropical cyclone activity
433 in the western North Pacific. *J. Meteorol Soc. Japan*, **79**, 23-25.

434 Yumoto, M., T. Matsuura, S. Iizuka, 2003: Interdecadal Variability of Tropical
435 Cyclone Frequency over the Western North Pacific in a High-Resolution
436 Atmosphere-Ocean Coupled GCM. *J. Meteorol Soc. Japan*, **81**,1069-1086.

437 Zhao, H., L. Wu, and W. Zhou, 2011: Interannual Changes of Tropical Cyclone
438 Intensity in the Western North Pacific. *Journal of the Meteorological Society of*
439 *Japan*, **89(3)**, 243-253, doi: 10.2151/jmsj.2011-305.

440

441

442

443

444

445

446

447

448

449

450 Table Captions

451 Table 1 Summary of numerical experiments conducted with the tropical cyclone
452 intensity model

453 Figure Captions

454 Figure 1 The annual unadjusted (solid) and adjusted (dashed) number of tropical cyclones
455 (TCs) reaching tropical storm strength in the Joint Typhoon Warning Center (JTWC)
456 best track dataset over the western North Pacific (WNP) during the period 1948-2010.
457 Where TC maximum wind speeds in the JTWC dataset prior to 1973 is adjusted with the
458 recently-used pressure-wind relationship as described in Emanuel (2005).

459 Figure 2 (a) Unadjusted (green) adjusted (black) and simulated (red) annual number of

460 Cat45 TCs in the JTWC dataset over the WNP basin. A 5-year running average is
461 applied to the time series. (b) Normalizations of adjusted (dashed) and simulated (solid)
462 annual number of Cat45 TCs over the WNP basin. The time series have been detrended
463 and a 5-year running average is also applied.

464 Figure 3 Spectral analysis of the annual number of the unadjusted (a), adjusted (b) and
465 simulated (c) Cat45 TCs during the period 1948-2010 in the WNP basin. The 95%
466 confidence levels with respect to the red noise spectrum are shown by the black dashed
467 line.

468 Figure 4 The climatological mean SST (dashed contours) and mean vertical wind shear (solid
469 contours) during the period 1948-2010 over the WNP basin. Dots represent locations of
470 the first occurrence of Cat45 TC intensity reported in the adjusted JTWC dataset. The
471 green box highlights location of the territory of Guam, where JTWC provides tropical
472 cyclone watches and warning prior to 1999.

473 Figure 5 (a) Time series of the normalized annual simulated Cat45 TC number in experiments
474 CTRL (solid line), V-Clim (dashed line with closed dots), VT-Clim (dashed line with
475 plus sign) and T-Clim (dashed line with open dots) during the period 1948-2010,
476 respectively; (b) the SST effect (dashed line with closed dots) and vertical wind shear
477 effect (dashed line with open dots) on the decadal variability of Cat45 TC frequency,
478 which can be examined by contrasting the experiments VT-Clim and V-Clim (T-Clim),
479 respectively. The solid line as shown in (b) also represents the simulated Cat45 TC
480 frequency from the CTRL experiment.

481 Figure 6 Time series of the normalized annual simulated Cat45 TC frequency for CTRL
482 (solid line) and the difference between the CTRL and VT-Clim experiments (dashed line)
483 (a), in which the environmental vertical wind shear and SST changed while the TC
484 tracks remain unchanged, indicating the combined effect of SST and vertical wind shear
485 on the decadal variability of Cat45 TC frequency. Similarly, (b) shows the time series of
486 the normalized annual simulated Cat45 TC frequency for two experiments CTRL (solid
487 line) and VT-Clim (dashed line), which indicates the effect of track changes on the
488 decadal variability of Cat45 TC frequency. See the details in text.

489 Figure 7 Composite difference of TC genesis frequency (*100) over the peak TC season

490 (July-September) between the positive and negative phases. The difference with shading
 491 is statistically significant at the 95% level.

492 Figure 8 The correlation between the adjusted Cat45 TC frequency over the WNP basin and
 493 SST over the peak TC season (July-September) for (a) the period 1965-2010 and (b) and
 494 1948-2010. The shaded areas indicate significant at the 95% confidence level.

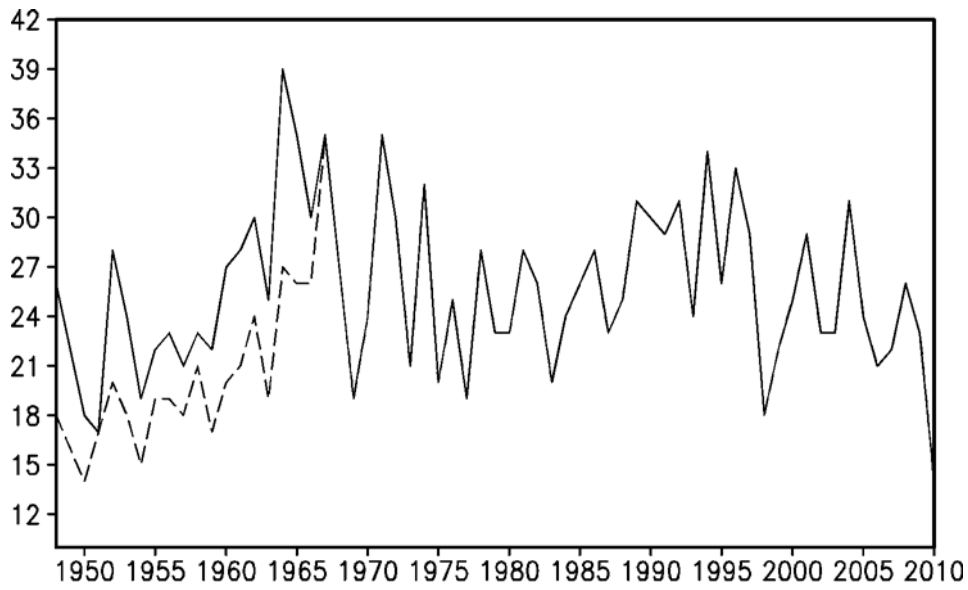
495 Figure 9 Difference of the wind fields (vectors; unit: m s⁻¹) at 850 hPa and SST (contours;
 496 interval for solid contours: 0.1°C) over the peak TC season (July-September). Only
 497 differences of wind field and SST above the 95% significance level are depicted by
 498 vectors and color shading, respectively.

499
 500
 501
 502
 503
 504
 505
 506
 507
 508
 509
 510

511 Table 1 Summary of numerical experiments conducted with the tropical cyclone
 512 intensity model

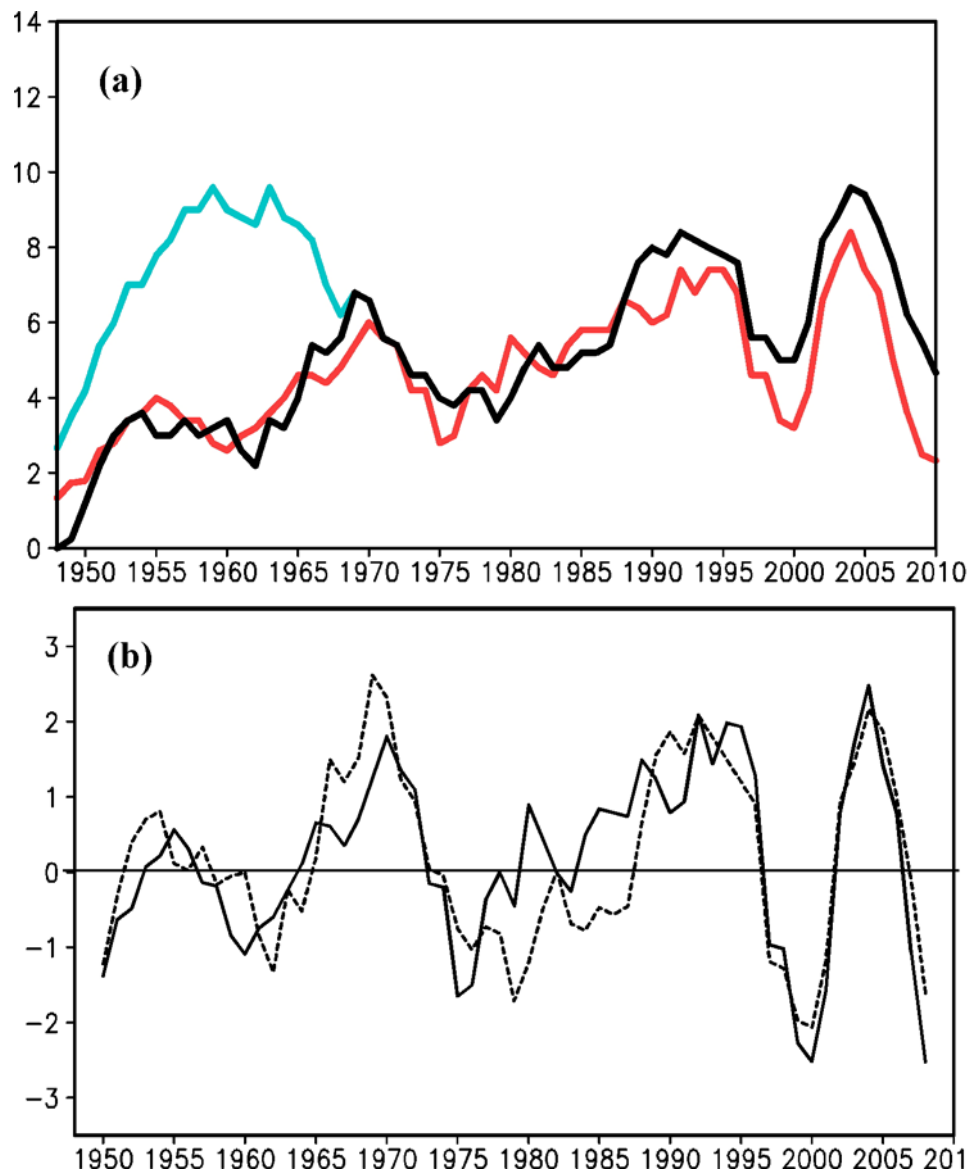
<i>Experiments</i>	<i>Simulation Description</i>
<i>CTRL</i>	Both of SST and vertical wind shear are observed from 1948 to 2010.
<i>T-Clim</i>	SST is observed in the climatological mean during 1948-2010, but vertical wind shear changes with the observation from 1965 to 2010.
<i>V-Clim</i>	Shear is observed in the climatological mean during 1948-2010, but SST changes with the observation from 1965 to 2010.
<i>VT-Clim</i>	Both of SST and vertical wind shear are set to be those observed in the climatological mean during 1948-2010.

513
 514

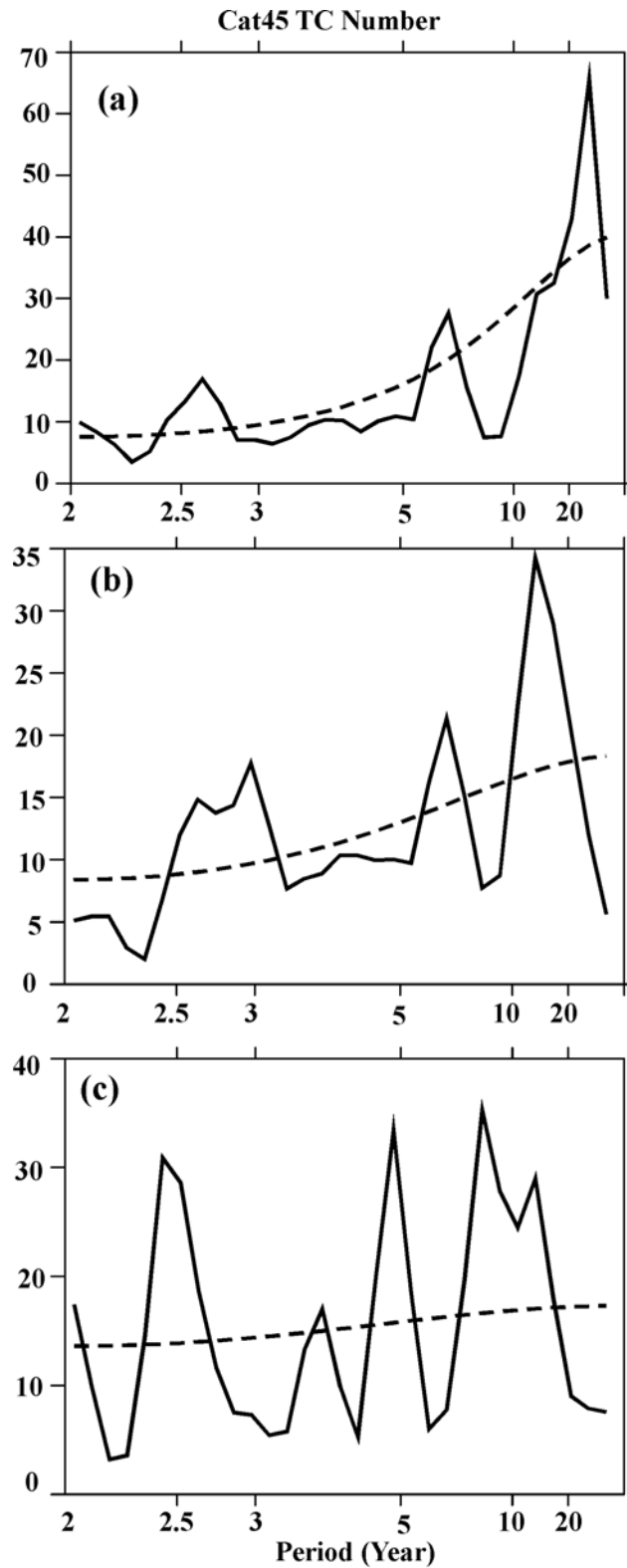


515
 516
 517
 518
 519
 520
 521
 522
 523

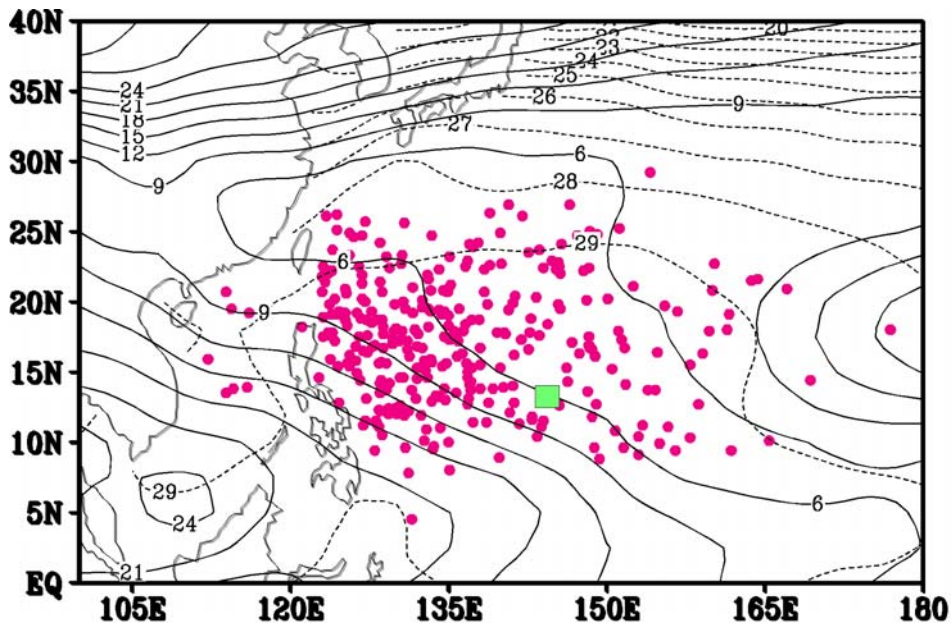
Figure 1 The annual unadjusted (solid) and adjusted (dashed) number of tropical cyclones (TCs) reaching tropical storm strength in the Joint Typhoon Warning Center (JTWC) best track dataset over the western North Pacific (WNP) during the period 1948-2010. Where TC maximum wind speeds in the JTWC dataset prior to 1973 is adjusted with the recently-used pressure-wind relationship as described in Emanuel (2005).



524
 525 Figure 2 (a) Unadjusted (green) adjusted (black) and simulated (red) annual number
 526 of Cat45 TCs in the JTWC dataset over the WNP basin. A 5-year running average is
 527 applied to the time series. (b) Normalizations of adjusted (dashed) and simulated
 528 (solid) annual number of Cat45 TCs over the WNP basin. The time series have been
 529 detrended and a 5-year running average is also applied.
 530

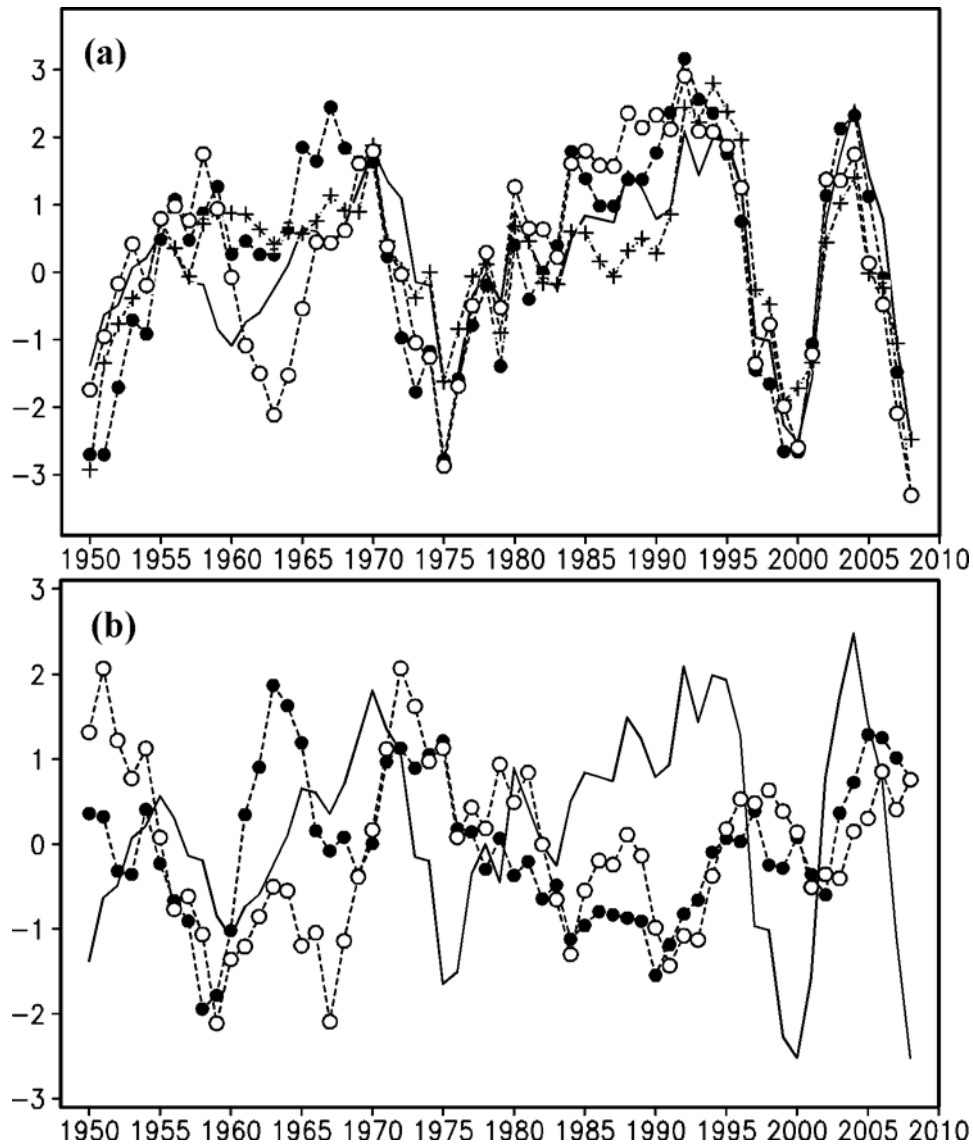


531
 532 Figure 3 Spectral analysis of the detrended annual number of the unadjusted (a),
 533 adjusted (b) and simulated (c) Cat45 TCs during the period 1948-2010 in the WNP
 534 basin. The 95% confidence levels with respect to the red noise spectrum are shown by
 535 the black dashed line.



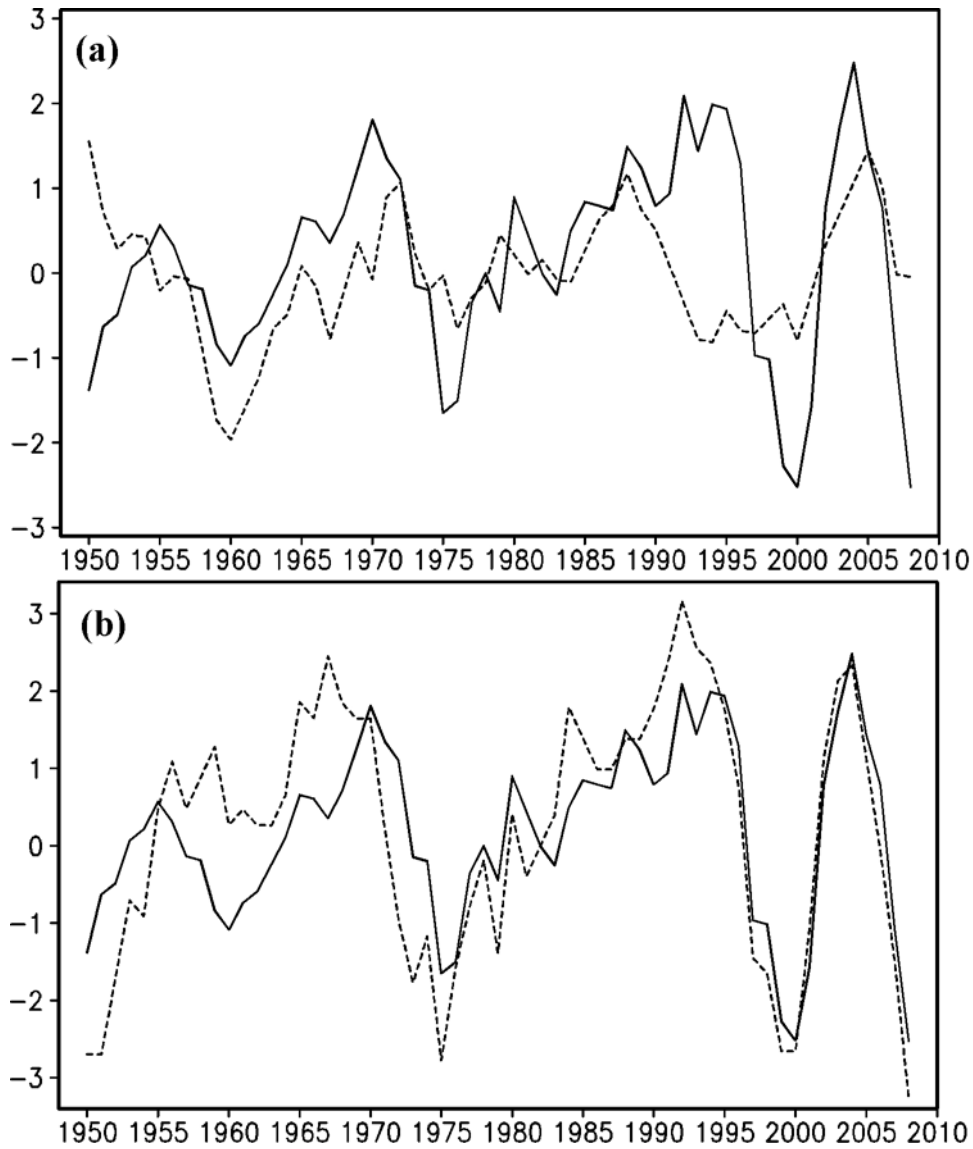
536

537 Figure 4 The climatological mean SST (dashed contours) and mean vertical wind
 538 shear (solid contours) during the period 1948-2010 over the WNP basin. Dots
 539 represent locations of the first occurrence of Cat45 TC intensity reported in the
 540 adjusted JTWC dataset. The green box highlights location of the territory of Guam,
 541 where JTWC provides tropical cyclone watches and warning prior to 1999.



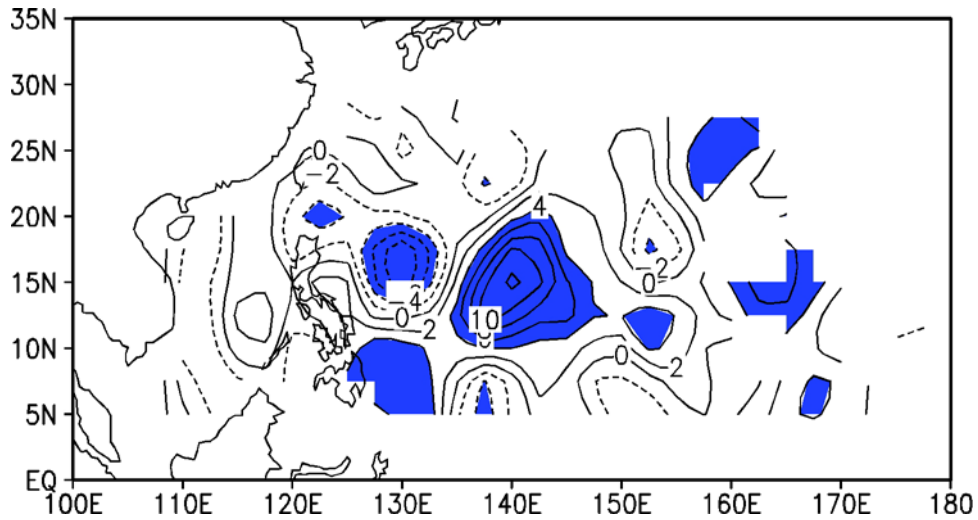
542
 543
 544
 545
 546
 547
 548
 549
 550
 551

Figure 5 (a) Time series of the normalized annual simulated Cat45 TC number in experiments CTRL (solid line), V_Clim (dashed line with closed dots), VT-Clim (dashed line with plus sign) and T-Clim (dashed line with open dots) during the period 1948-2010, respectively; (b) the SST effect (dashed line with closed dots) and vertical wind shear effect (dashed line with open dots) on the decadal variability of Cat45 TC frequency, which can be examined by contrasting the experiments VT-Clim and V-Clim (T-Clim), respectively. The solid line as shown in (b) also represents the simulated Cat45 TC frequency from the CTRL experiment.



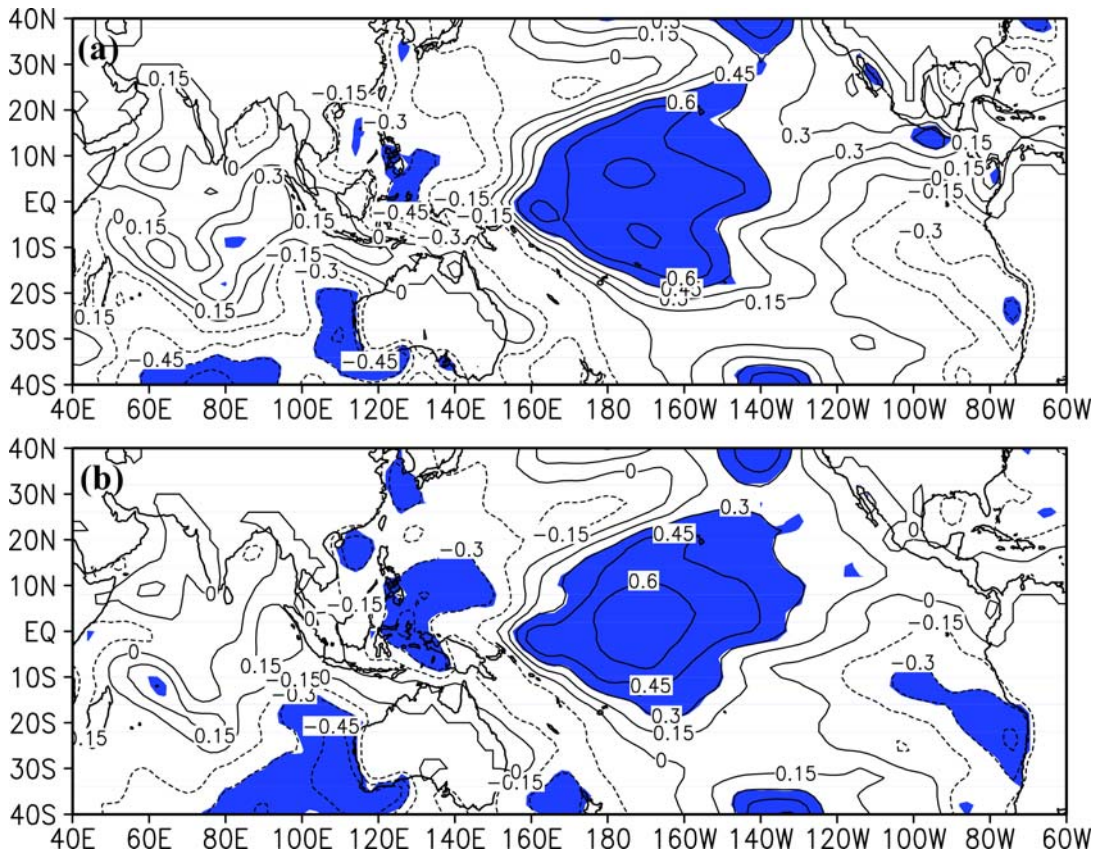
552
 553
 554
 555
 556
 557
 558
 559
 560
 561
 562
 563

Figure 6 Time series of the normalized annual simulated Cat45 TC frequency for CTRL (solid line) and the difference between the CTRL and VT-Clim experiments (dashed line) (a), in which the environmental vertical wind shear and SST changed while the TC tracks remain unchanged, indicating the combined effect of SST and vertical wind shear on the decadal variability of Cat45 TC frequency. Similarly, (b) shows the time series of the normalized annual simulated Cat45 TC frequency for two experiments CTRL (solid line) and VT-Clim (dashed line), which indicates the effect of track changes on the decadal variability of Cat45 TC frequency. See the details in text.



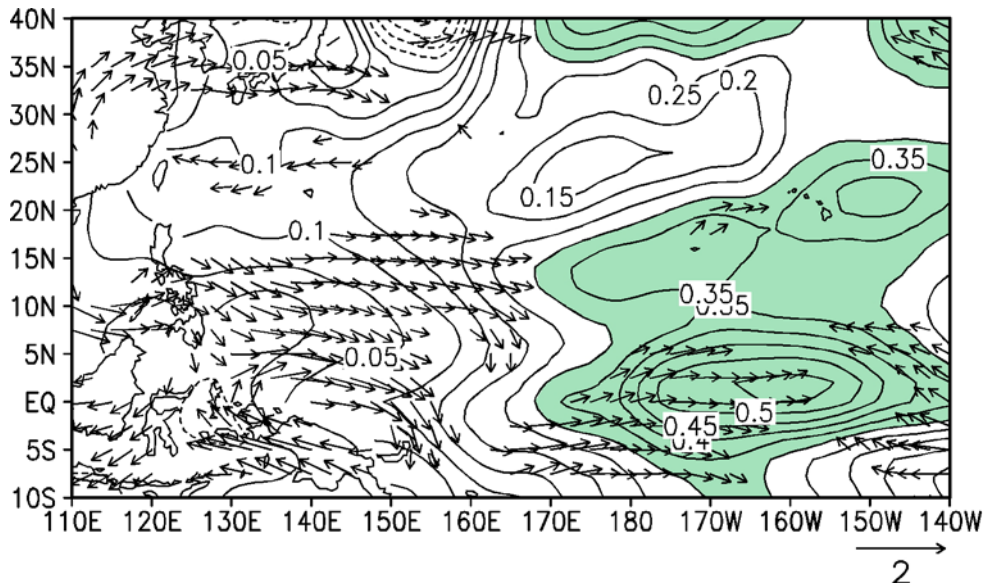
564

565 Figure 7 Composite difference of TC genesis frequency (*100) over the peak TC
 566 season (July-September) between the positive and negative phases. The difference
 567 with shading is statistically significant at the 95% level.



568

569 Figure 8 The correlation between the adjusted Cat45 TC frequency over the WNP
 570 basin and SST over the peak TC season (July-September) for (a) the period
 571 1965-2010 and (b) and 1948-2010. The shaded areas indicate significant at the 95%
 572 confidence level.



573

574 Figure 9 Difference of the wind fields (vectors; unit: m s^{-1}) at 850 hPa and SST
 575 (contours; interval for solid contours: 0.1°C) over the peak TC season
 576 (July-September). Only differences of wind field and SST above the 95% significance
 577 level are depicted by vectors and color shading, respectively.